

Published in POLYMER

Polymer 53 (2012) 2705-2716

Study of morphology and crystal growth behaviour of nanoclay-containing biodegradable polymer blend thin films using atomic force microscopy

Thomas Malwela^{1,2} and Suprakas Sinha Ray^{1,2}*

¹*DST/CSIR Nanotechnology Innovation Centre, National Centre for Nano-Structured Materials, Council for Scientific and Industrial Research, Pretoria 0001, South Africa*

²*Department of Chemical Technology, University of Johannesburg, Doornfontein 2018, Johannesburg, South Africa*

Abstract

Thin films of unmodified and nano-clay modified polylactide/poly(butylene succinate) (PLA/PBS) blends were prepared on a glass substrate with a spin coater. The morphology and crystal growth behaviours for the films, crystallized at different temperatures, were visualized with atomic force microscope (AFM). AFM images showed that the size of the dispersed PBS-phase was reduced on the addition of 2 wt% clay to the PLA/PBS blend, and the size of the dispersed phase increases with the further addition of clay. Transmission electron microscopy studies indicated that this behaviour was due to the preferential location of silicates in the PBS phase than in the PLA phase. A similar effect of clay to the blend thin films on the dispersed phase and the crystalline morphology were observed when annealed at 60 °C and 120 °C. However, at 60°C the addition of clay to the blend quenched the growth of edge-on lamellae. The crystalline morphologies at 120 °C were dominated by edge-on lamellae grown around the PBS phase to form spherulites. Morphologies of thin films crystallized at 120 °C from melt were dominated by the flat-on lamellae, while the ones crystallized at 70 °C from melt were dominated by the edge-on lamellae. The degree of clay silicate dispersion in the blend matrix was characterized by X-ray diffraction. These results show how the crystallization temperatures and the addition of the clay-particles influence the morphology of the thin films.

*Corresponding author. Fax: +27 12 841 2229; E-mail: rsuprakas@csir.co.za

1. Introduction

The blends of polylactide (PLA) and poly(butylene succinate) (PBS) have received considerable research attention because of their potential applications as advanced environmental-friendly packaging materials [1–3]. The soft biodegradable plastic PBS generally blended with PLA to improve the brittleness of PLA, which is one of its main drawbacks, that limits its applications [4]. However, when PLA and PBS are blended together, the resulting blend shows phase-separated morphology with poor interfacial adhesion and hence, poor properties of blend. Researchers are using various compatibilizers, such as PLA-co-PBS, to improve the compatibility between phases [5]. Reactive processing is another frequently used technique for the production of compatibilized blends with much improved properties [6]. This technique has also been used for the production of compatibilized PLA/PBS blends [7].

In recent years, researchers have shown that organically modified nano-clay (or organoclay) particles can play an alternative route to manipulate the interfacial properties of a variety of immiscible polymer blends [8–10]. For example, Sinha Ray et al. have shown the role of organoclay interfacial activity on immiscible PP/PS blends [11]. Transmission electron microscopy (TEM) at high magnification revealed clear localization of intercalated silicate layers at the interface between the phases. Additional measurements showed a decrease in interfacial tension, which is a clear indication of interfacial compatibilization of the blend [11]. In their subsequent studies, they investigated extensively the effect of the miscibility of the organic modifier with the polymer matrices, as well as the effect of the initial interlayer spacing of the silicate galleries, on the morphology and properties of the immiscible PC/PMMA [12–14], PP/PBSA [15], PP/PBS [16], and PLA/PBSA [17] blend systems.

Recently, a couple of studies have been reported on the organoclay-containing PLA/PBS blend systems [3, 18–20]. Bhatia et al. investigated the thermal, rheological, morphological, and mechanical properties of unmodified and organoclay-modified PLA and PBS blends [18]. On the other hand, Chen and Yoon [19] studied thermal stability and thermo-mechanical properties of PLA/PBS/clay composites containing Cloisite[®]25A (C25A) and twice-functional organoclay (TFC). Results showed significant improvements in properties when TFC was used to prepare composites with PLA/PBS. According to the authors, such improvements were due to the highly dispersed morphology of intercalated silicate layers in the blend matrix and the increased interaction between the polymer matrices and the silicate surfaces through chemical reactions. However, all reported works are in the bulk state, prepared either by melt-blending or solution casting.

Currently, polymer thin films have received great research attention due to their important role in a variety of high-technological applications, such as coatings, adhesion, electronics, and so on [21]. Literature search show that studies on thin films of neat polymers [22–26] and on polymer blends thin films [27–29] has been conducted. If the polymer matrices confined in thin film geometry, such that surface area to volume ratio is very high, surface effect will dominate and the phase separation will be different from that for the bulk samples. Using nano-clay particles in the phase separated PLA/PBS

blend thin films, a number of phase-separated structures, which will have great importance for many applications ranging from lithography to drug-released capsules, can be fine-tuned. Therefore, in this article, we present our first results on the morphology of nanoclay-modified PLA/PBS blend thin films and our understanding of the morphology obtained using AFM. To the best knowledge of our literature search, no work has been presented on PLA/PBS blend thin films containing nanoclays.

Over the last few years, AFM has become established as one of the most popular tools to investigate the topology and physical characteristics of polymeric materials [30]. In addition to its extremely high resolution, AFM has the added benefit of simplicity in terms of sample preparation as compared to other microscopy techniques such as electron microscopy. In this work, the tapping mode was used to capture both height and phase images of unmodified and nanoclay-modified PLA/PBS blend thin films. The height images are used to study the phase separated morphology of blend thin films because height images generate the true three-dimensional topography of the sample surface, whereas phase images are used to understand the surface crystallization behaviour of unmodified and nanoclay-modified PLA/PBS blend thin films upon annealing (both *ex-* and *in-situ*) at different temperatures because phase images are useful for getting sharp contrast of the features.

2. Experimental details

2.1. Materials

Both polymers used in this study were commercial products. The PLA, with *D* content of 1.1-1.7% was obtained from Unitika Co. Ltd., (Japan). According to the supplier, it had a weight average molecular weight, $M_w = 200$ kg/mol, density = 1.25 g/cm³ (ASTM 1238), glass transition temperature, $T_g = \sim 60^\circ\text{C}$ and melting temperatures, $T_m = \sim 170^\circ\text{C}$. On the other hand, the PBS, with the designation BIONOLLE #1020, was obtained from Showa High Polymer (Japan). According to the supplier, low molecular weight PBS extended with 1,6-diisocynatahexane, it had $M_w = 180$ kg/mol, density = 1.22 g/cm³ (ASTM 1238), $T_g = -42^\circ\text{C}$ and T_m 's = 115°C . Before use, PLA was dried at 60°C under vacuum for 36 h, whereas, PBS was dried at 60°C under vacuum for 12 h.

The organoclay, Cloisite[®]30B (C30B) was purchased from Southern Clay Products, USA. According to the supplier, the pristine montmorillonite (MMT) was modified with 30 wt% of methyl tallow bis(2-hydroxyethyl) quaternary ammonium salt.

2.2. Preparation of C30B-containing PLA and PBS nanocomposites using melt-blending

Nanocomposites of PLA and PBS containing 5 wt% C30B were prepared by first melting each polymer matrix and then mix with C30B for 10 min in Thermohaake twin-rotors mixer at two different sets of temperatures (185°C for PLA and 135°C for PBS) and a rotor speed of 60 rpm. The

composites were then compression moulded using a carver laboratory press at the same processing temperature for 10 min into sheets of 0.5 mm and then cooled at room temperature.

2.3. Preparation of unmodified and 2 wt% C30B-containing PLA and PBS blends using melt-blending

Blends of PLA and PBS with one weight composition (70/30 = PLA/PBS) were prepared under the same conditions by first melting the polymers and then mix with C30B (different weight percent, from 1 to 5 wt%) for 10 min in Thermohaake twin-rotors mixer (Polylab system) at 185°C (set temperature) and a rotor speed of 60 rpm. The blends were then compression moulded using a Carver laboratory press at 185°C for 10 min into sheets of 0.5 mm thick and then cooled at room temperature. Samples were then freeze-fractured to expose the surface for morphology analysis.

2.3. Preparation of unmodified and 2 wt% C30B-containing PLA and PBS blends using solution-blending

The solution of neat PLA and PBS were first prepared by dissolving them in chloroform (volume was constant) at room temperature (~25 °C). The blend (70PLA/30PBS) was then prepared by dissolving the PLA and PBS separately in chloroform at room temperature, and then the solutions were mixed and sonicated for 15 min, and subsequently cast on a glass dish. Blend thin film with 2 wt% C30B loading was prepared using the same method as described above; by separately dissolving PLA, PBS, and dispersing C30B in chloroform (total volume was constant for all samples).

2.4. Preparation of unmodified and C30B-containing PLA and PBS blends thin films

Thin films of neat PLA and PBS were prepared by dissolving them in chloroform (volume was constant) at room temperature (~25 °C). Thin films were prepared on a glass substrate using a spin coater that was ramped at 500 rpm for 10 s and subsequently ramped at 1000 rpm for 20 s. The samples were allowed to dry in air at room temperature. The blend (70PLA/30PBS) was prepared by dissolving the PLA and PBS separately in chloroform at room temperature, and then the solutions were mixed and sonicated for 15 min. The solution mixture was used to prepare thin films on a glass substrate using a spin coater. Blend thin films with different loadings of C30B (1–5 wt%) were prepared by separately dissolving PLA and PBS and dispersing C30B in chloroform (total volume was constant for all samples). The solutions were then mixed and sonicated for 15 min, and then thin films of various composites on a glass substrate were prepared by spin-casting. The thickness of various thin films (1.3–1.5 μm) was measured directly by cross-sectioned analysis using focused-ion beam scanning electron microscopy (Zeiss, Auriga FIB-SEM).

2.2. Characterization

The degree of dispersion of silicate layers in the polymer matrix was investigated by means of TEM (JEOL, JEM 1250), operated at an accelerating voltage of 80 kV. The ultrathin sections (the edges of

the sample sheets) with a thickness of 150 nm were microtomed at $-80\text{ }^{\circ}\text{C}$ using a Reichert Ultracut cryo-ultramicrotome without staining.

The surface morphology of unmodified and C30B-modified PLA/PBS blends, prepared using three different methods, was studied by means of field emission scanning electron microscopy (SEM, Auriga[®] from Carl Zeiss). To avoid charging, all samples were carbon coated before being subjected to SEM study.

The X-ray diffraction (XRD) measurements were conducted using Phillips X'pert X-ray diffractometer operated at 45.0 kV and 40.0 mA with $\text{CuK}\alpha$ radiation.

The flow behaviours of neat PLA, PBS, unmodified and C30B-modified PLA/PBS blends in molten states were studied by an Anton-Paar stress-strain controlled rheometer model MCR-501 with a parallel plate (PP-25) configuration. Samples prepared using melt-blending were used for this study. To do the dynamic oscillatory measurements, one should first determine the amplitude of oscillation in the linear viscoelastic region where any structural change is supposed to be reversible. Hence, the strain amplitude sweep experiments of all samples were performed at $175\text{ }^{\circ}\text{C}$ with a constant angular frequency (ω) = 6.28 rad/s in the varying strain window 0.01–100%. The frequency sweep experiments were carried out at the same temperature with a strain amplitude of 2% in the frequency range 100–0.01 rad/s, at $175\text{ }^{\circ}\text{C}$.

A multimode AFM (Nano Scope Version (R) IV) using 0.5–2.0 Ωcm phosphorous (n) doped Si tip with a radius curvature of less than 10 nm (Veeco Instruments) was used to study the surface morphology of the unmodified and C30B-modified PLA/PBS blend thin films. The RTESPW tip mounted on a 125 μm long cantilever with the spring constant of 40 N/m was employed for tapping mode experiments. Samples were imaged using a scan rate of 0.5 Hz, and the tip frequencies were ranged from 280–310 kHz. Three different areas on each as-prepared and dried thin film of unmodified and C30B-modified blends were imaged. Only representative images are reported in this article. The height images of various samples were used for the particle size distribution of dispersed PBS phase using ImageJ[®] software.

To study the effect of the annealing temperature on surface morphology and crystal growth, all samples were annealed at two different temperatures of $60\text{ }^{\circ}\text{C}$ and $120\text{ }^{\circ}\text{C}$ for 1 h. After 1 h, each sample was immediately quenched in liquid nitrogen to freeze the morphology and then scanned as soon as possible before significant morphological change could occur. *In situ* crystalline morphology studies were performed with AFM equipped with hot-stage scanner. Thin films were heated to melt at $180\text{ }^{\circ}\text{C}$ and then rapidly cooled down to the crystallization temperatures of $120\text{ }^{\circ}\text{C}$ and $70\text{ }^{\circ}\text{C}$. The images were captured at these crystallization temperatures after allowing them to crystallize for 20 min.

3. Results and discussion

3.1. Dispersed clay morphology of PLA and PBS nanocomposites

On the basis of Flory-Huggins theory, one can describe the compatibilization effect of two immiscible polymers A and B by the addition of a third component, S. Therefore, in a three component (per unit volume) system of S with polymers A and B, the free energy of mixing is given by:

$\Delta G_{\text{mix}} = \Delta G_{\text{AS}} - \Delta G_{\text{BS}} - \Delta G_{\text{AB}}$, where the subscripts identify the interacting pairs.

According to the above equation, when both polymers in a blend have a strong interaction with the filler surface, the interaction parameters (ΔG_{AS} and ΔG_{BS}) of polymers A and B with the surface of S will be negative, and thermodynamically driven compatibility will be likely to occur between the polymers A and B.

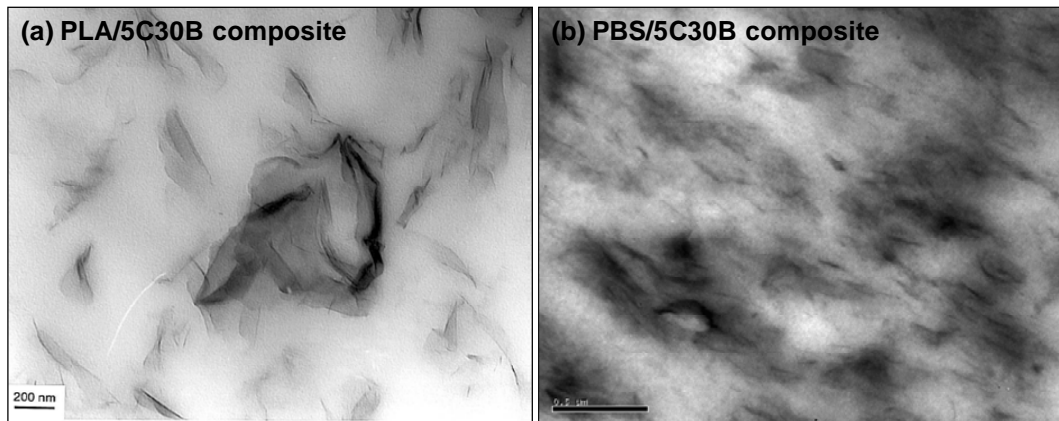


Fig. 1. Bright field transmission electron microscopy (TEM) images of: (a) PLA/5C30B and (b) PBS/5C30B composites.

In the case of clay-containing polymer composites, the degree of interaction of the clay surface with the polymer matrix is generally determined by the extent of intercalation of polymer chains into the two dimensional silicate galleries of clay. Now to determine the degree of interaction of C30B surface with each homopolymer matrix, 5 wt% of C30B was separately melt-mixed with 95 wt% of PLA and PBS, and TEM study was conducted. Parts (a) and (b) of Fig. 1, respectively, show the bright field TEM images of PLA/5C30B and PBS/5C30B composites. TEM images show that clay particles are very nicely dispersed in the PBS matrix compared to the PLA matrix. As the degree of dispersion of clay particles in a polymer matrix is directly related to the favourable interaction between the organoclay surface and polymer matrix, the results indicate that the C30B surface has a more favourable interaction with the PBS matrix compared to the PLA matrix.

3.2. Structure and morphology of unmodified and C30B-modified PLA/PBS blend thin films

Taking into consideration the known ability of C30B to form an intercalated structure with both PLA and PBS matrices, the aim of this section is to find out whether the addition of C30B could have an effect on the surface morphology of immiscible PLA/PBS blends prepared using three different methods, such as melt-mixing, solution- and spin-casting. Fig. 2 shows the surface morphology of PLA/PBS blends and their composites containing 2 wt% C30B, prepared using three different methods. Clearly, the processing method has a strong effect on the surface morphology of PLA/PBS blend. On the other hand, 2 wt% C30B has a significant effect on the morphology of PLA/PBS blend prepared using all three different methods. Particularly, in the case of 2 wt% C30B containing blend composite thin film (thickness $\sim 1.5 \mu\text{m}$); it is very difficult to differentiate the phase separated morphology under examined magnification.

To have insight into the morphology of unmodified and C30B-modified PLA/PBS blend thin films, the tapping-mode AFM analyses were carried out to understand the molecular scale morphology of PLA/PBS blend thin films in the presence and absence of C30B. Recently, AFM was established as one of the most popular tools to investigate the topology and physical characteristics of polymeric materials at the molecular level [30].

Fig. 3 shows the $5 \times 5 \mu\text{m}^2$ height images (left side) and corresponding three dimensional (3D) topographies (right side) of **as-prepared** unmodified and various C30B-modified PLA/PBS blend thin films. The size distributions of dispersed PBS phase in various blends are also presented in Fig. 3 (middle). The height image and 3D-topography of unmodified PLA/PBS blend clearly show a two-phase morphology (PLA as matrix and PBS as dispersed phase), indicating the expected immiscibility of the two components. The size distribution analysis reveals that the average diameter of the dispersed phase is about 257.5 nm from a total number (N) of 93 dispersed PBS domains. With the addition of 1 wt% C30B, the average diameter of the dispersed phase increases to 290 nm with a decrease in the number of dispersed domains to 78. The addition of 2 wt% C30B significantly reduced the diameter of the dispersed phase to 211 nm and increased the number of domains to 163 within the measured area of $5 \times 5 \mu\text{m}^2$. With the addition of 3 wt% C30B, the number and diameter of the dispersed domains remain almost the same with 2 wt% C30B-modified blend. However, with further increase of C30B loading to 4 wt%, the diameter of the dispersed phase increased and the number of dispersed domains was decreased. In the case of 5 wt% C30B-modified blend, the diameter of the dispersed domains significantly increased and revealed quite a pronounced phase-separated morphology compared to unmodified PLA/PBS blend.

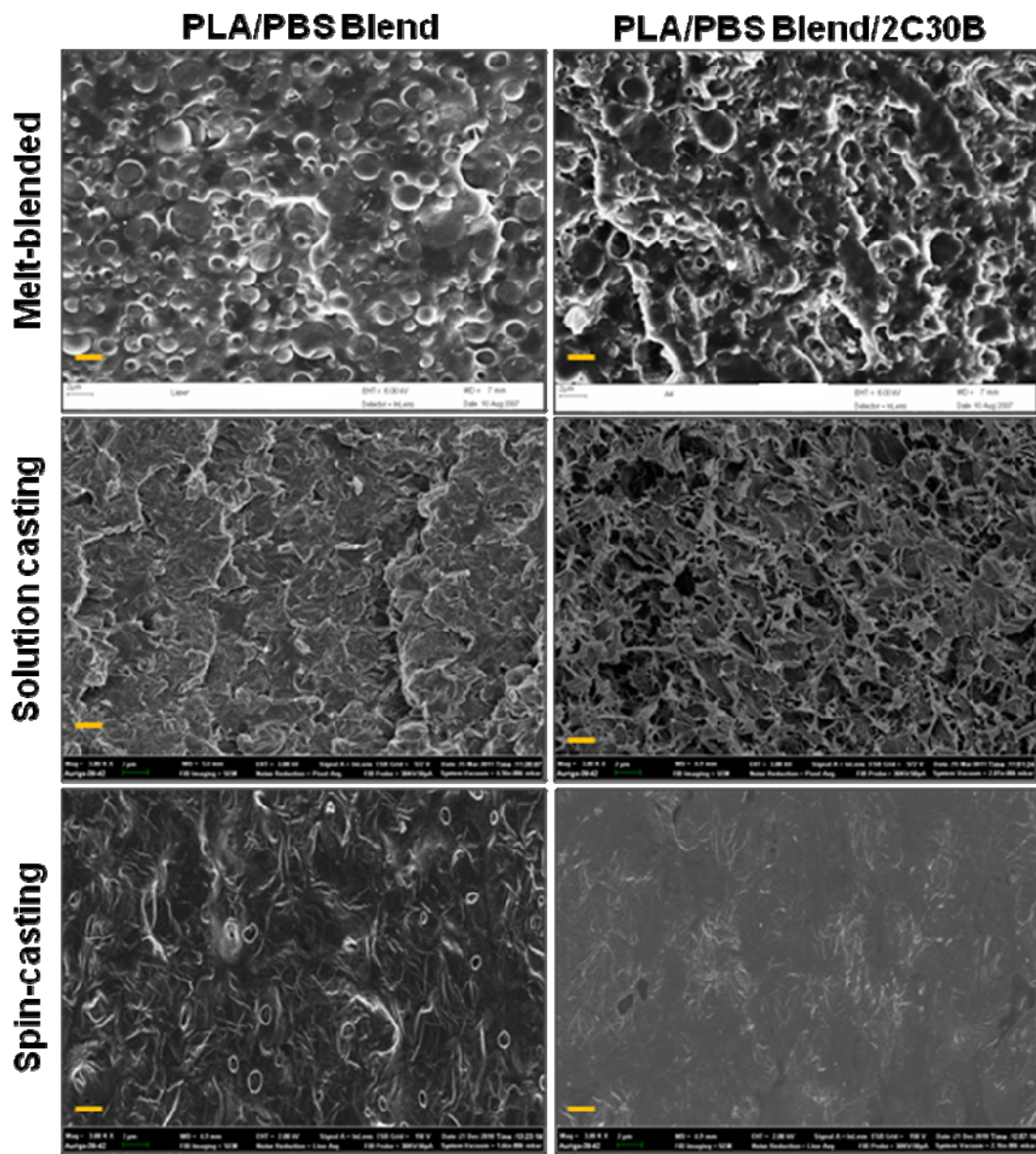


Fig. 2. Scanning electron microscope images of unmodified and 2 wt% C30B-modified PLA/PBS blends prepared using three different methods.

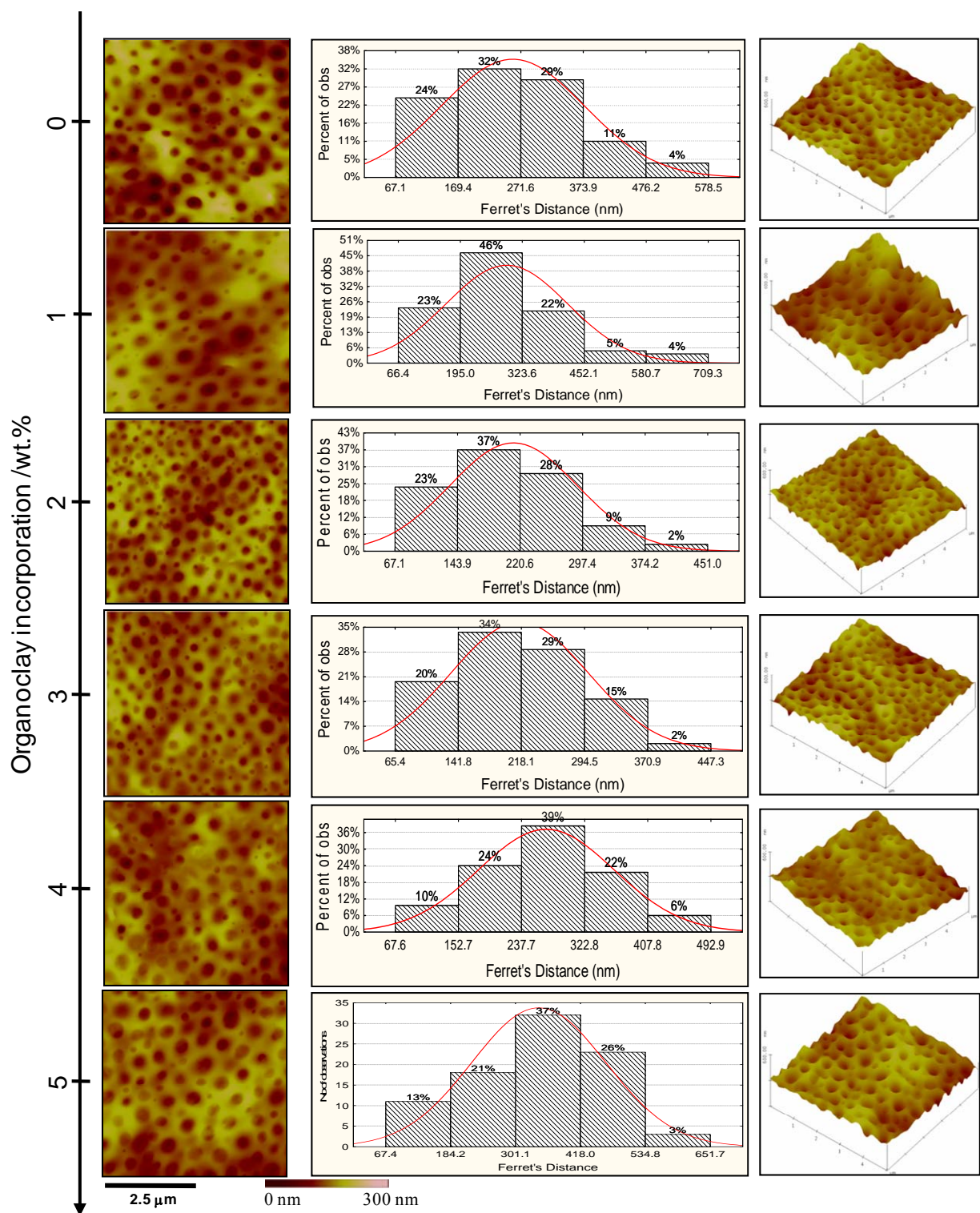


Fig. 3. The $5 \times 5 \mu\text{m}^2$ AFM height images (left side), the size distributions of dispersed PBS phase (middle) and corresponding three dimensional (3D) topographies (right side) of **as-prepared** unmodified and various C30B-modified PLA/PBS blend thin films.

The above results indicate the preferential location of the silicate particles in the PBS matrix, and the change in the rheological behaviours of the dispersed phase may be the possible reason for observed morphology with increase C30B loading. Up to the addition of 2 wt% of C30B, most of the silicate layers went to the PBS matrix as PBS has a much higher favourable interaction with C30B than PLA (refer to Fig. 1, TEM images) and increased the viscosity of the dispersed phase. Under such circumstances, the viscosity ratio of the PBS phase and the PLA phase increased, and as a result, the diameter of the dispersed PBS phase decreased in the case of PLA/PBS/2C30B composite thin film. In case of the bulk sample a co-continuous like morphology was obtained, see Fig. 2. The situation remains almost the same up to the addition of 3 wt% C30B. With the further addition of C30B in PLA/PBS blend, the viscosity ratio of the two phases started to decrease as the PBS phase has no free volume to accommodate extra silicate particles and the silicate particles started to move to the PLA matrix. As a result the viscosity ratio between phases again decreased and hence, so did the dispersed phase diameter. In the case of PLA/PBS/5C30B blend, the viscosity ratio of the two phases is much higher than that of the unmodified PLA/PBS blend. For this reason, the diameter of the dispersed PBS phase is much higher in the case of 5 wt% C30B-modified PLA/PBS blend than unmodified PLA/PBS blend.

To support the above conclusion, the melt-state complex viscosity of neat PLA, PBS, unmodified, and various C30B-modified PLA/PBS blends were measured at 175 °C, and the results are presented in Fig. 4. Although these samples were prepared using a melt-blending method, the presented results give an indication about the effect of adding C30B to the blend viscosity. It is clear from the figure that 1 wt% C30B addition has no effect on the viscosity of PLA/PBS blend. The difference in melt-state viscosity of PLA/PBS/2C30B and PLA/PBS/3C30B composites was not that much. For this reason, there is almost no significant difference in observed morphology. However, the viscosity of PLA/PBS blend significantly increased after the addition of 5 wt% C30B.

To further support the conclusions made on the basis of SEM, AFM, and viscosity data, the dispersion characteristic of the silicate layers in the blend matrix was carried out by means of XRD. The XRD patterns of the C30B powder, unmodified and C30B-modified PLA/PBS blends are presented in Fig. 5. In the XRD patterns of both PLA/PBS/1C30B and PLA/PBS/2C30B composites, the characteristic peak of C30B almost disappears suggesting that the ordered structure of C30B is completely destroyed. Such an observation indicates that either the silicate layers are highly delaminated in the case of PBS matrix leading to the formation of delaminated composite thin films or the absence of peak may be due to the effect of dilution. However, a broad C30B characteristic peak appears at 4.2° in the XRD pattern of PLA/PBS/3C30B composite, indicating that the silicate layers started to intercalate by the PLA chains. With further increase of the C30B loading into the PLA/PBS blend, the characteristic C30B peak position moved towards the high diffraction angle. Therefore, the above results indicate that dispersion of nanoclay particles in the individual polymer matrix and the ultimate viscosity play significant roles to control the thin-film morphology.

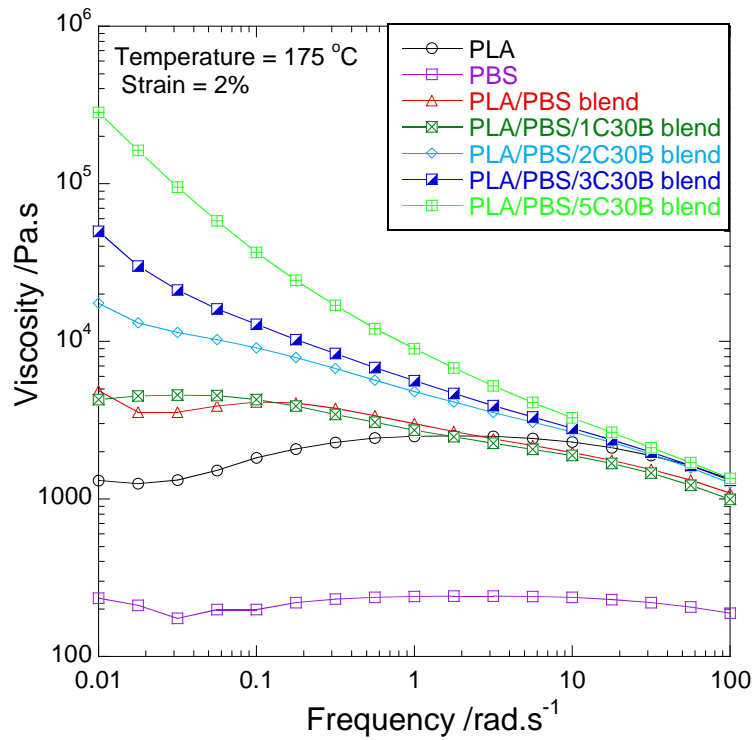


Fig. 4. Melt-state complex viscosity of neat PLA, PBS, unmodified, and various C30B-modified PLA/PBS blends at 175 °C. Here all samples were prepared using melt-blending technique.

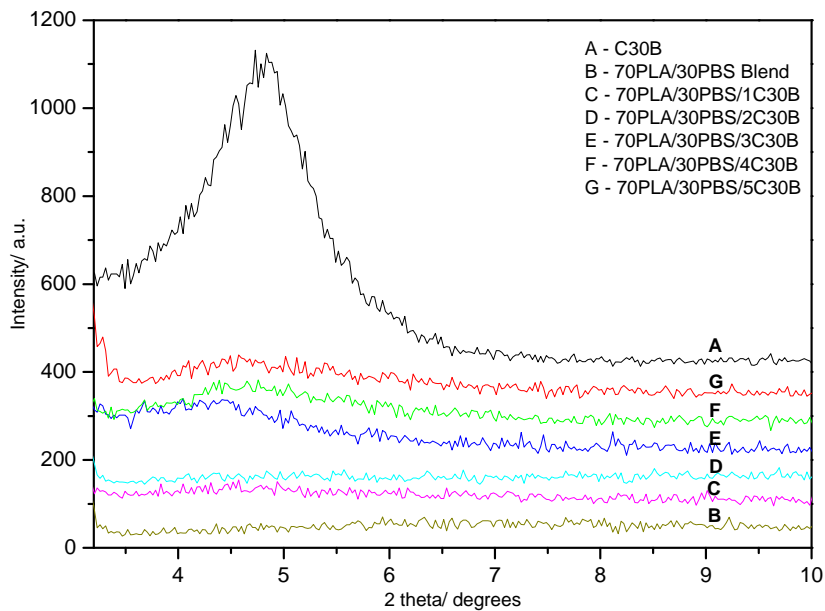


Fig. 5. X-ray diffraction patterns of unmodified and various C30B-modified PLA/PBS blends.

3.3. Crystal growth behaviour of unmodified and C30B-modified PLA/PBS blend thin films

The crystal growths of unmodified and C30B-modified PLA/PBS blend thin films were investigated with both *ex situ* and *in situ* AFM. *Ex situ* studies were carried out on as-prepared thin films, annealed at 60 °C and 120 °C and quenched in liquid nitrogen before being subjected to AFM studies. Fig. 6 represents AFM phase images of as-prepared unmodified and C30B-modified PLA/PBS blend thin films. The morphology of unmodified blend thin films has two phases, the dispersed phase and the main phase. The dispersed phase is associated with the PBS phase and the main phase is PLA. The introduction of C30B from 1–5 wt% to PLA/PBS blend affected the size and distribution of particle size of the dispersed (PBS) phase as discussed in Fig. 3. At this point, as-prepared morphologies of the unmodified PLA/PBS blend thin films did not exhibit any crystalline structure. This is obvious because as-prepared PLA thin films do not exhibit any crystalline morphology since PLA is the main phase and difficult to crystallize at room temperature. The modification with 1–5 wt% C30B to the PLA/PBS blend did not initiate the crystal growth as well.

To examine the influence of annealing temperatures on unmodified and C30B-modified PLA/PBS blend thin films, samples were annealed at 60 °C for 1 h (for PBS phase to crystallize) and quenched in liquid nitrogen before being subjected to AFM study. Fig. 7 shows the AFM phase images of unmodified and C30B-modified PLA/PBS blend thin films annealed at 60 °C for 1 h. The morphology of unmodified PLA/PBS blend thin films in Fig. 7(a) shows the edge-on lamellae, which started to grow around the edges of the dispersed (PBS) phase. However, the addition of 1 wt% C30B quenched the growth of these edge-on lamellae as shown in Fig. 7(b). Further addition of C30B to the blend from 2–5 wt% continued to quench the growth of edge-on lamellae. In this temperature, PBS is expected to crystallize while PLA is not. The edge-on lamellae grown around the dispersed phase can be associated with the PBS crystals, and therefore this observation suggests that the presence of C30B at 60 °C prevents the growth of edge-on structures of the dispersed phase. This may be due to the high degree of intercalation of PBS chains into the silicate galleries, which actually inhibits the crystal growth [31].

Unmodified and C30B-modified blend thin films were further annealed at 120 °C for 1 h (for PLA phase to crystallize) and quenched in liquid nitrogen. Fig. 8 illustrates the AFM phase images of unmodified and C30B-modified PLA/PBS blend thin films annealed at 120 °C for 1 h. The AFM images of unmodified PLA/PBS blend presented in Fig. 8(a) is composed of the edge-on lamellae grown around the dispersed phase. The growth formed spherulites around the dispersed phase, and their centers coincide with that of the dispersed phase. A close inspection shows some edge-on lamellae grown within the dispersed phase. When 1 wt% C30B was added, the size of the dispersed phase distribution looks similar to the unmodified blend but the edge-on lamellae look thinner (refer to Fig. 8(b)). On the addition of 2 wt% C30B, the size of the dispersed phase became smaller and uniformly distributed throughout the sample surface as shown in Fig. 8(c). The edge-on lamellae were grown around the dispersed phase but with thinner lamellae.

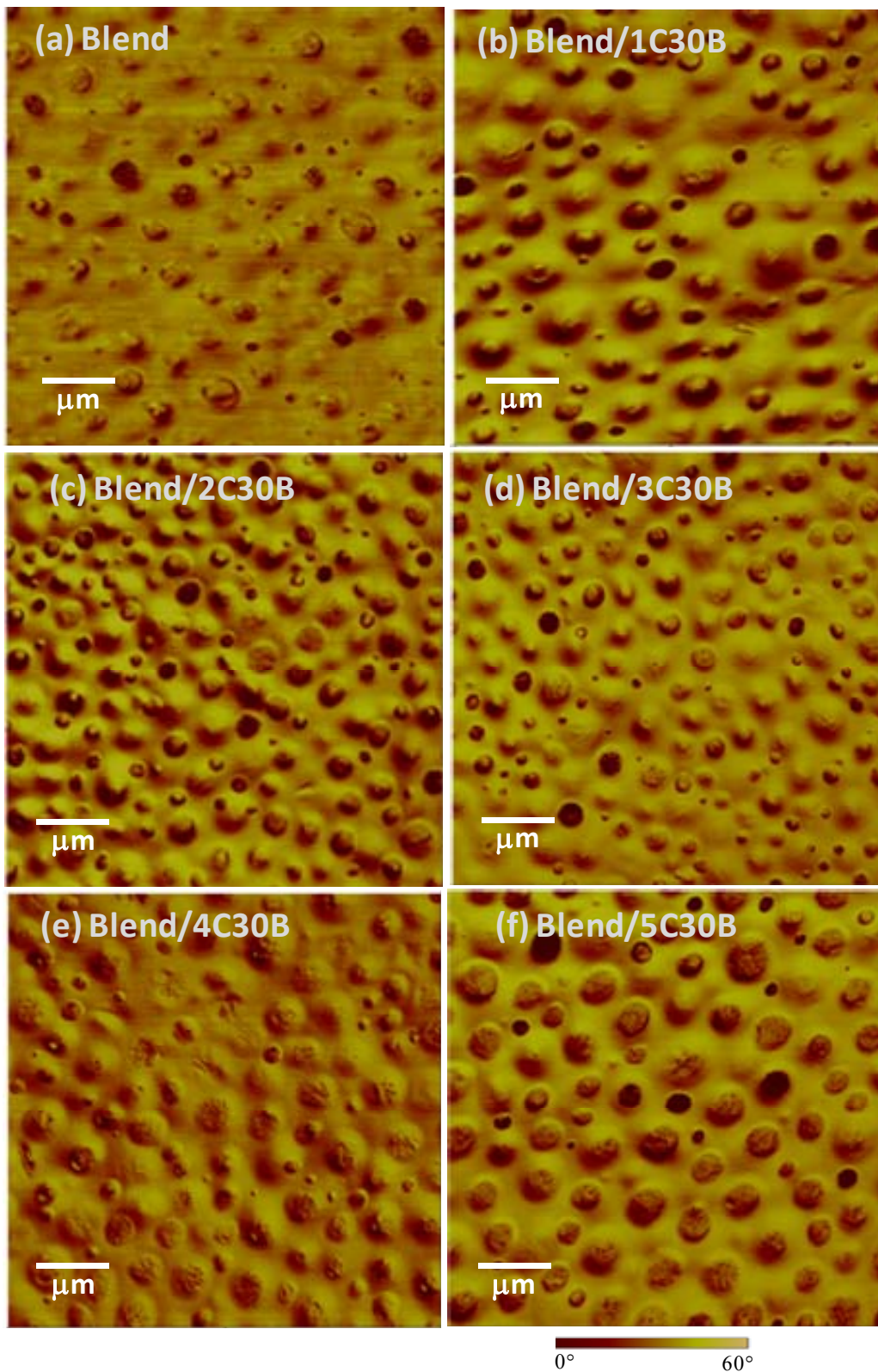


Fig. 6. The $5 \times 5 \mu\text{m}^2$ AFM phase images of as-prepared unmodified and various C30B-modified PLA/PBS blends.

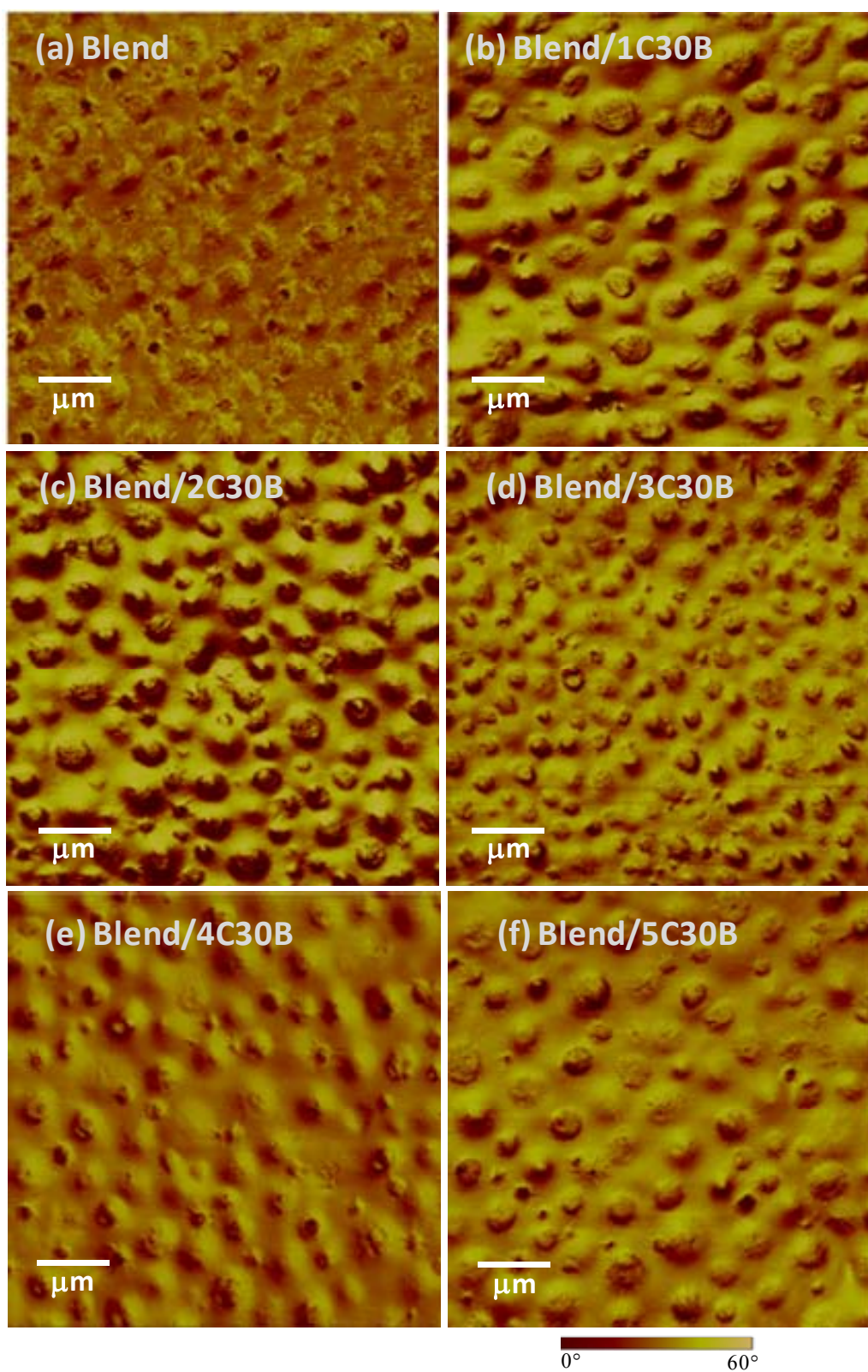


Fig. 7. The $5 \times 5 \mu\text{m}^2$ AFM phase images of unmodified and various C30B-modified PLA/PBS blends annealed at 60°C for 1 h quenched in liquid nitrogen.

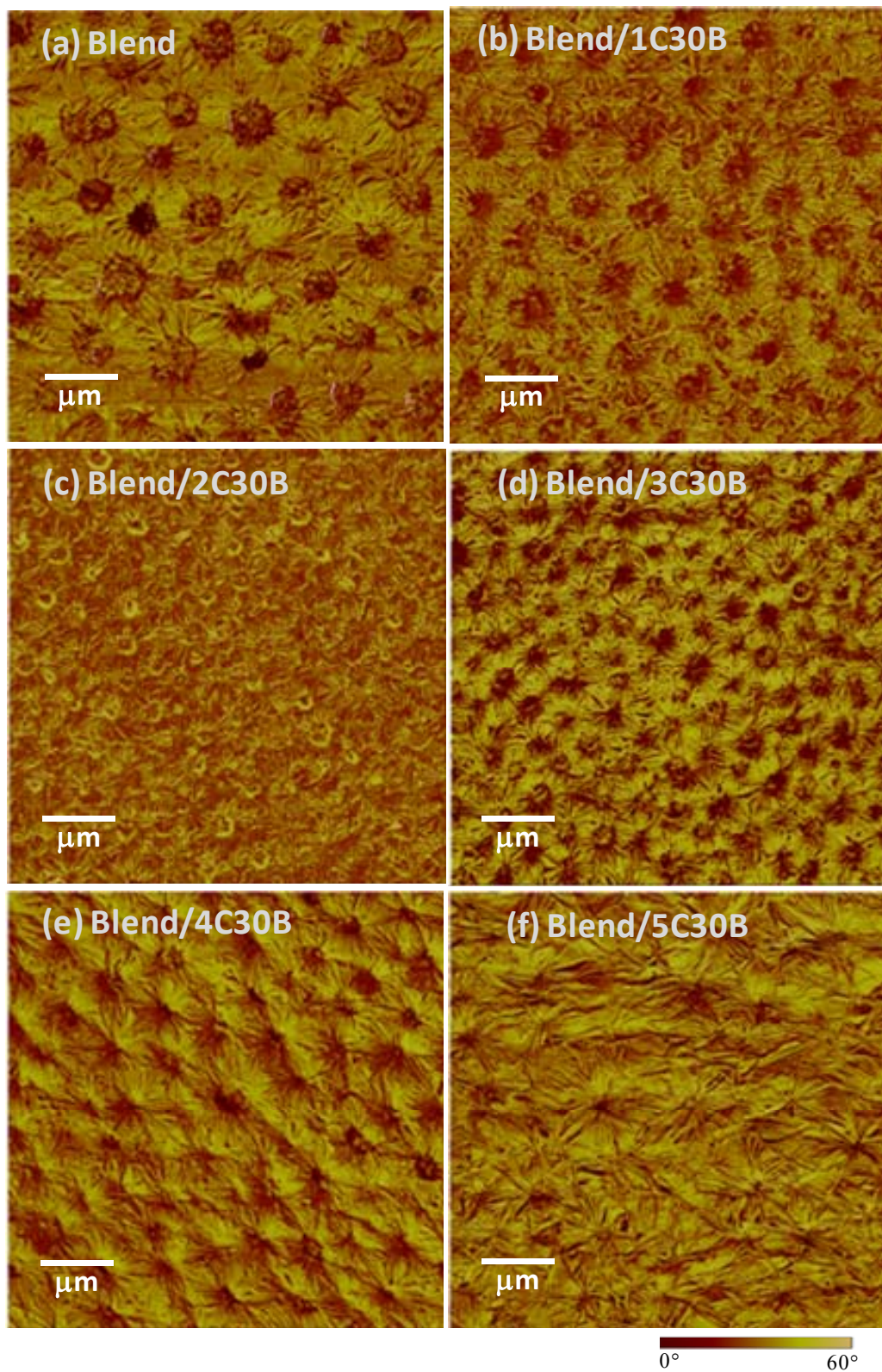


Fig. 8. The $5 \times 5 \mu\text{m}^2$ AFM phase images of unmodified and various C30B-modified PLA/PBS blends annealed at 120°C for 1 h and quenched in liquid nitrogen.

Further addition of C30B (3 wt%, refer to Fig. 8(d)) formed the crystalline morphology that looks similar to that of PLA/PBS blend with 2 wt% C30B. However, the thicknesses of the edge-on lamellae seem to have slightly increased compared to the PLA/PBS blend with 2 wt% C30B loading. This argument can be clearly seen in Fig. 8(e), where the addition of 4 wt% C30B produced a morphology with much thicker edge-on lamellae. The initial development of flat-on lamellae can be observed and become pronounced when 5 wt% C30B was added to PLA/PBS blend (see Fig. 8(f)). The morphology has both edge-on and flat-on lamellae. At this point, the dispersed phases could not be identified.

The unmodified PLA/PBS blend thin films at lower annealing temperatures (60 °C) exhibited the development of edge-on lamellae around dispersed phases. The addition of C30B hindered this growth. This suggests that the clays, which are mainly situated on and around the PBS phase, quenched the crystal growth. When the annealing temperature was increased to 120 °C, the crystalline morphology of unmodified PLA/PBS blend thin films is composed of fully developed edge-on lamellae compared to Fig. 8(a). At this temperature, PBS is in the molten state while PLA crystallizes. The PBS edge-on structures that grow before melt formed the scaffold for PLA crystals. During annealing, the temperature on the film surface was lower than in the polymer/substrate interface. As a result, very fast nucleation took place on the film surface leading to the growth of edge-on lamellae [4]. The addition 1 and 2 wt% reduced both the size of the dispersed phase and the thickness of edge-on lamellae, while the increase in lamellae thickness was observed on the addition of 3, 4, and 5 wt%. The development of flat-on lamellae started when 4 wt% C30B was added and became more visible when 5 wt% was added. In this case, higher contents of C30B quench the growth of edge-on lamellae and therefore allowing flat-on lamellae to grow. It was noted that the influence of the clays on lamellae thickness was related to the effect it had on the phase separations of the blend. In the beginning most of the clays were intercalated in the PBS phase than in PLA phase. As the clay content increases, some clay particles intercalate in the PLA phase and therefore act as nucleating sites which promote the heterogeneous nucleation and is associated with the growth of flat-on lamellae. This effect is clearly demonstrated in Fig. 8(e).

In situ crystal growths of unmodified and C30B-modified PLA/PBS blend thin films were investigated with AFM equipped with hot-stage. The films were heated to melt at 180 °C and then rapidly cooled to the crystallization temperature of 120 °C and 70 °C. Fig. 9 depicts the AFM phase images of unmodified and C30B-modified PLA/PBS blend thin films crystallized at 120°C for 20 min from melt. The crystalline morphology of unmodified PLA/PBS blend thin film in Fig. 9(a) mainly has flat-on lamellae with “hard-to-indentify” edge-on lamellae. In the presence of 1 wt% C30B, the crystalline morphology was dominated by edge-on lamellae and few flat-on lamellae were observed, see Fig. 9(b). The image in Fig. 9(c) indicates that the addition of 2 wt% C30B produced the morphology having both flat-on and edge-on lamellae. Similar morphology was seen in Figs. 9(d) and 9(e) for the addition of 3 and 4 wt% C30B, respectively. Fig. 9(f) represents the morphology of PLA/PBS blend with 5 wt% C30B in which the morphology contains both flat-on and edge-on lamellae. Some of the flat-on lamellae folded up to form flower-like structures.

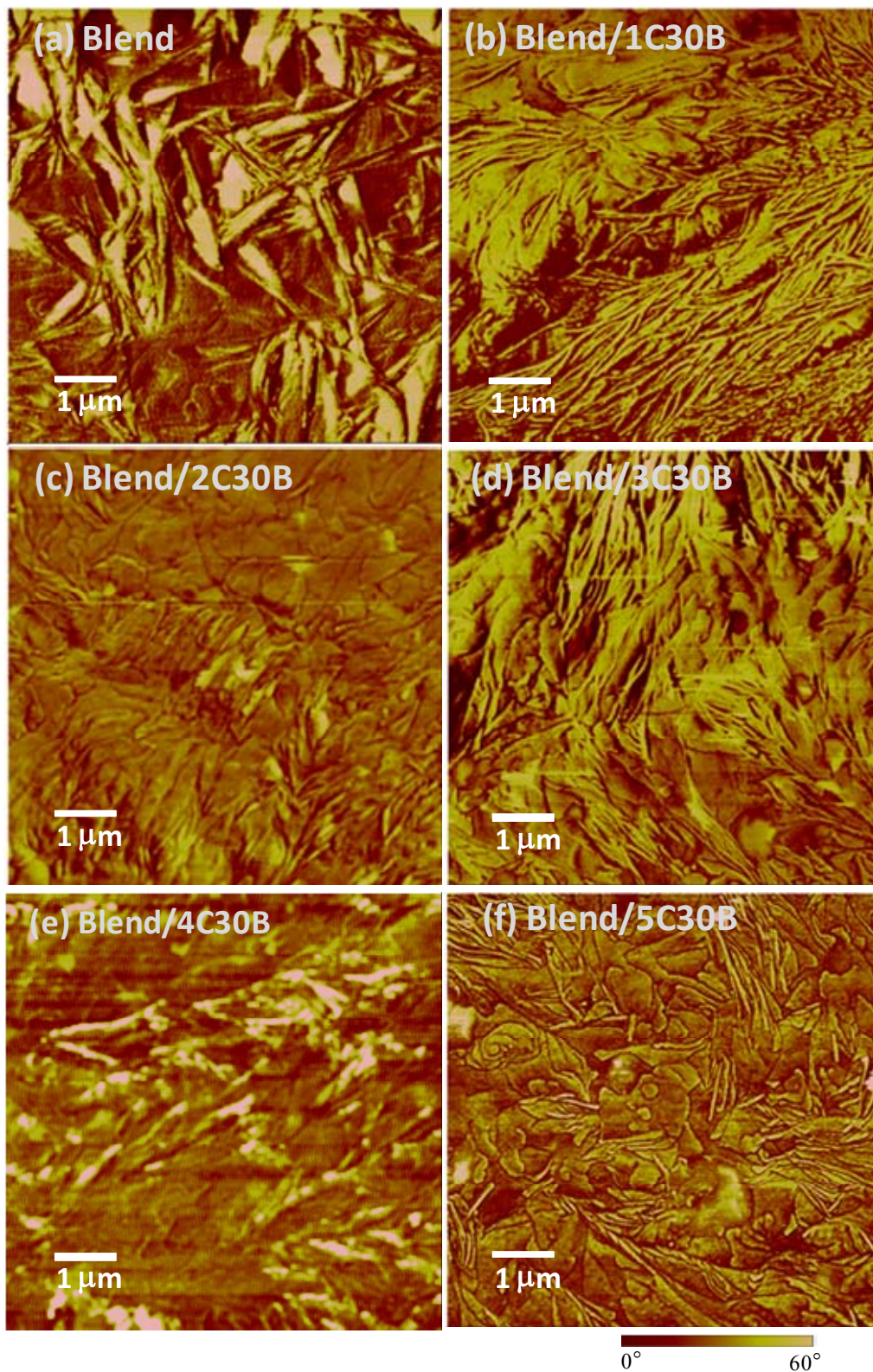


Fig. 9. The $5 \times 5 \mu\text{m}^2$ in situ AFM phase images of unmodified and various C30B-modified PLA/PBS blends crystallized at $120 \text{ }^\circ\text{C}$ for 20 min from melt at $180 \text{ }^\circ\text{C}$.

In an unmodified blend thin film, crystallization at 120 °C from melt at 180 °C favoured the growth of flat-on lamellae, which is associated with the heterogeneous nucleation [4]. Thus at higher temperatures, heterogeneous nucleation took place faster and quenched the other modes of crystallization. The inclusion of C30B promotes the growth of edge-on lamellae. The effect of the clays is different from what was observed when the samples were annealed at 120 °C from room temperature. The difference could be the result of the fact that at 180 °C, both PLA and PBS were in the molten state and the polymer chains were completely unfolded. It therefore provided the opportunity for the intercalated silicate layers to uniformly distribute throughout the thin film. When the films were quickly cooled down to 120°C, the PBS phase remained in the molten state while some of the clays were trapped in PLA phase as it crystallized. This brought the balance competition between the homogeneous and heterogeneous nucleation. Another explanation would be the fact that the arrangement of polymer chains from melt is different than the ones viewed when annealing from room temperature. During annealing, the ordering of polymer chains is influenced by the pre-existed amorphous state, while at melt, polymer chains completely unfold and start afresh to arrange when cooling to 120 °C.

Fig. 10 illustrates the AFM phase images of unmodified and C30B-modified PLA/PBS blend thin films crystallized at 70°C for 20 min from melt at 180 °C. Unmodified PLA/PBS blend thin film in Fig. 10(a) is dominated by the edge-on lamellae with hardly noticeable flat-on lamellae. In this case, the lower crystallization temperature (70°C) favours the growth of edge-on lamellae. This could be due to the fact that during rapid cooling to 120°C, heterogeneous nucleation slightly occurred first but was quenched by the subsequent dominance of homogeneous nucleation as the film cooled to 70°C. Fig. 10(b) shows PLA/PBS blend modified with 1 wt% C30B having a morphology that is dominated by the edge-on lamellae. The addition of 2 wt% C30B in Fig. 10(c) produced the crystalline morphology having both edge-on and flat-on lamellae. A similar effect is observed in Fig. 10(e). In the presence of 3 wt% C30B (Fig. 10(d)), the morphology is dominated by flat-on lamellae. Similar behaviour is observed in Fig. 10(f). This observation indicates that the increase in clay content coupled with the crystallization of PBS at lower crystallization temperatures promote very efficient heterogeneous nucleation leading to the growth of flat-on lamellae.

Crystal growth observed from annealing favoured the growth of edge-on lamellae. The growth started at the edges of the PBS phases. Lower temperatures are expected to favour fast nucleation, which is associated with the growth of edge-on lamellae [4]. In this study, the thin films were annealed on a hot-plate in open air. The surface was cooled down and hence gave the opportunity for the homogeneous nucleation to take place quickly and quench the heterogeneous nucleation. Crystallization at 120°C from melt favoured flat-on lamellae. This is attributed to higher temperatures, which promote heterogeneous nucleation. However, at 70 °C, the co-crystallization of PLA and PBS influence crystalline morphology as the clay content increases. The increase in heterogeneous nucleation was observed.

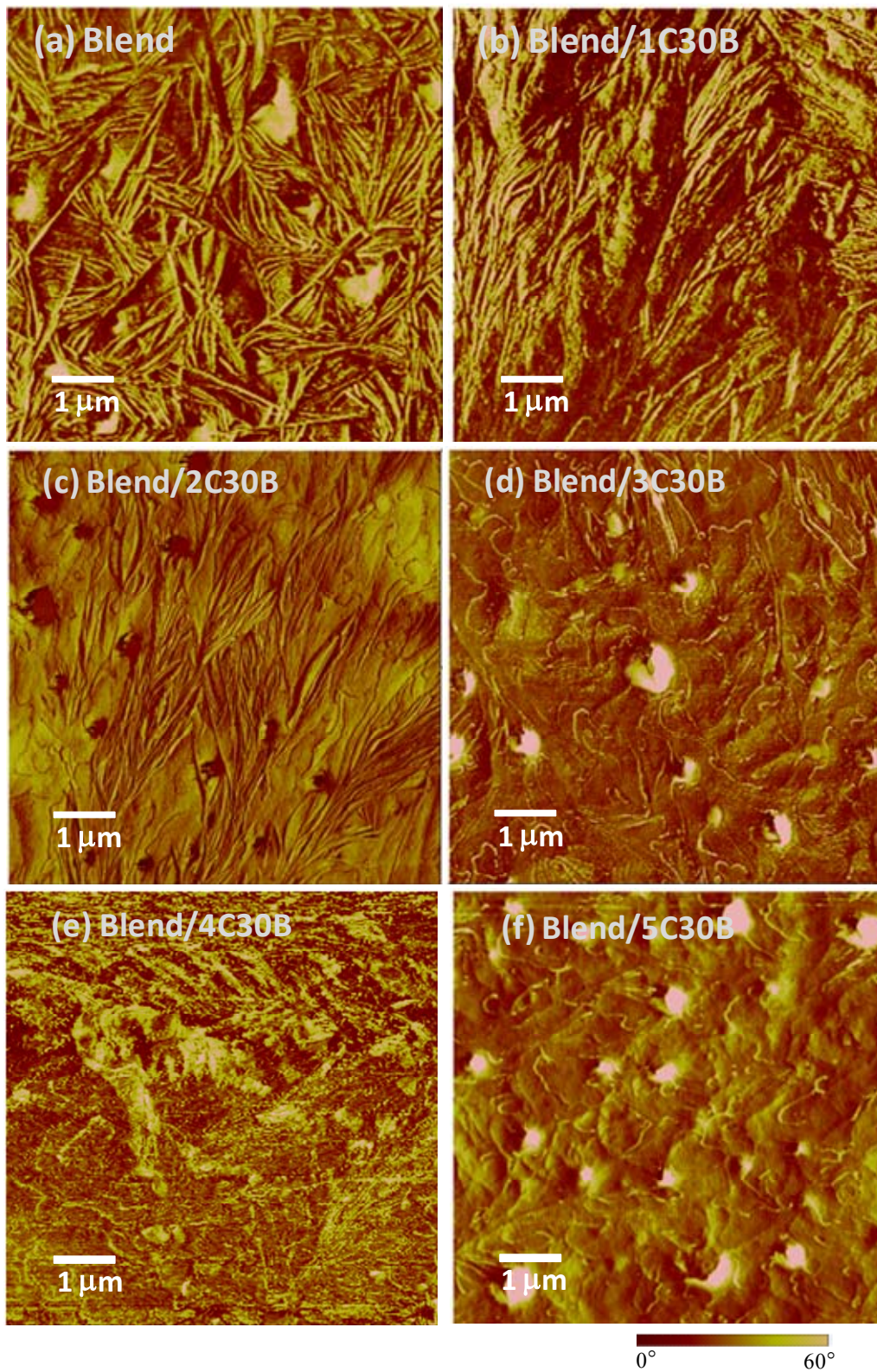


Fig. 10. The $5 \times 5 \mu\text{m}^2$ in situ AFM phase images of unmodified and various C30B-modified PLA/PBS blends crystallized at 70°C for 20 min from melt at 180°C .

4. Conclusions

The addition of C30B clay-particles influenced the size of the dispersed phase in the PLA/PBS blends. The clay-particles of C30B were found to disperse better in the PBS matrix than in the PLA matrix. This was associated with the degree of dispersion of clay particles in the polymer matrix, which is related to the interactions between the organoclay surface and the polymer matrix. C30B surfaces have more favourable interactions with the PBS matrix compared to the PLA matrix. This effect was also seen on the AFM morphologies of PLA/PBS blends, in which the addition of 2 wt% C30B indicated that most of the silicate layers may went in the PBS matrix and increased the viscosity of the dispersed phase. Further addition of C30B shows that some of the silicates moved to the PLA matrix due the lack of space in PBS matrix. Crystallizing thin films by annealing favoured the development of edge-on lamellae. This was attributed to lower temperatures in which homogeneous nucleation is faster than the heterogeneous nucleation. Crystallizing thin films from melt gave more preference to the development of flat-on lamellae due to higher temperatures in which heterogeneous nucleation takes place faster than homogeneous nucleation.

Acknowledgement: The authors would like to thank DST and CSIR for financial support and V. Ojijo for valuable comments.

References

- [1] Sinha Ray S, Bousmina M. Biodegradable polymers and their layered silicate nanocomposites: in greening the 21st century materials world. *Prog Mater Sci* 2005; 50: 962–79.
- [2] Auras R, Harte B, Selke S. An overview of polylactides as packaging materials. *Macromol Biosci* 2004;4:835–64.
- [3] Bhatia A, Gupta RK, Bhattacharya SN, Choi HJ. Compatibility of biodegradable poly (lactic acid) (PLA) and poly (butylene succinate) (PBS) blends for packaging application. *Korea-Australia Rheo J* 2007;19:125–31
- [4] Chuai C, Zhao N, Li Shu, Sun B. Study on PLA/PBS blends. *Adv Mater Res* 2011;197–198:1149–52.
- [5] Yu L, Dean K, Li L. Polymer blends and composites from renewable resources. *Prog Polym Sci* 2006;31:576–602.
- [6] Oyama HT. Super-tough poly(lactic acid) materials: Reactive blending with ethylene copolymer. *Polymer* 2009;50:747–51.
- [7] Harada M, Ohya T, Iida K, Hayashi H, Hirano K, Fukuda H. Increased impact strength of biodegradable poly(lactic acid)/poly(butylene succinate) blend composites by using isocyanate as a reactive processing agent. *J Appl Polym Sci* 2007;106:1813–20.
- [8] Khatua BB, Lee DJ, Kim HY, Kim JK. Effect of organoclay platelets on morphology of nylon-6 and poly(ethylene-*ran*-propylene) rubber blends. *Macromolecules* 2004; 37: 2454–59.
- [9] Li YJ, Shimizu H. Novel morphologies of poly(phenylene oxide) (PPO)/polyamide6 (PA6) blend nanocomposites. *Polymer* 2004; 45:7381–88.
- [10] Kim HB, Choi JS, Lee CH, Lim ST, John MS, Choi HJ. Polymer blend/organoclay nanocomposite with poly(ethylene oxide) and poly(methyl methacrylate). *Euro Polym J* 2005;41:679–85.
- [11] Sinha Ray S, Pouliot S, Bousmina M, Utracki LA. Role of organically modified layered silicate as an active interfacial modifier in immiscible polystyrene/polypropylene blends. *Polymer* 2004; 45: 8403–13.
- [12] Sinha Ray S, Bousmina M. Effect of organic modification on the compatibilization efficiency of clay in an immiscible polymer blend. *Macromol Rapid Commun* 2005; 26: 1639–46.
- [13] Sinha Ray S, Bousmina M. Compatibilization efficiency of organoclay in an immiscible polycarbonate/poly(methyl methacrylate) blend. *Macromol Rapid Commun* 2005; 26: 450–55.
- [14] Sinha Ray S, Maazouz A, Bousmina M. Morphology and properties of nanocomposites based on immiscible polycarbonate/poly(methyl methacrylate) blend and organoclay. *Polym Eng Sci* 2006;46:1120–29.
- [15] Sinha Ray S, Bandyopadhyay J, Bousmina M. Effect of organoclay on the morphology and properties of poly(propylene)/poly[(butylene succinate)-co-adipate] blends. *Macromol Mater Eng* 2007; 292: 729–47.
- [16] Gcwabaza T, Sinha Ray S, Focke WW, Maity A. Morphology and properties of nanostructured materials based on polypropylene/poly(butylene succinate) blend and organoclay. *Euro Polym J* 2009;45:353–67.

- [17] Ojijo V, Cele H, Sinha Ray S. Morphology and Properties of Polymer Composites Based on Biodegradable Polylactide/Poly[(butylene succinate)-*co*-adipate] Blend and Nanoclay. *Macromol Mater Eng* 2011;296:865–77
- [18] Bhatia A, Gupta R, Bhattacharya SN, Choi HJ. An investigation of melt rheology and thermal stability of poly(lactic acid)/ poly(butylene succinate) nanocomposites. *J Appl Polym Sci* 2009; 114: 2837–47.
- [19] Chen GX, Yoon JS. Thermal stability of poly(L-lactide)/poly(butylene succinate)/clay nanocomposites. *Polym Degrad Stabil* 2005;88:206–11.
- [20] Zhao L, Li Y, Shimizu H. Structural control of co-continuous poly(L-lactide)/poly(butylene succinate)/clay nanocomposites. *J Nanosci Nanotechnol* 2009; 9: 2772–76.
- [21] Schonherr H, Frank CW. Ultrathin films of poly(ethylene oxides) on oxidized silicon. 1. Spectroscopic characterization of film structure and crystallization kinetics. *Macromolecules* 2003;36:1188–98 and references cited therein.
- [22] Taguchi K, Miyayi H, Izumi K, Hoshino A, Miyamoto Y, Kokawa R. Growth shape of isotactic polystyrene crystals in thin films. *Polymer* 2001; 42; 7443 – 7447.
- [23] Gan Z, Abe H, Doi Y. Biodegradable poly(ethylene succinate) (PES). 1. Crystal growth kinetics and morphology. *Biomacromolecules* 2000; 1; 704 – 712.
- [24] Abe H, Kikkawa Y, Inoue Y, Doi Y. Morphological and kinetics analyses of regime transition for poly[(s)-lactide] crystal growth. *Biomacromolecules* 2001; 2; 1007 – 1041.
- [25] Maillard D, Prud'homme R.E. Crystallization of ultrathin films of polylactides: from chirality to lamella and twisting. *Macromolecules* 2008; 41; 1705 – 1712.
- [26] Yang J, Liao Q, Zhou J, Jiang X, Wang X, Zhang Y, Jiang S, Yan S, Li L. What determines the lamellar orientation on the substrates? *Macromolecules* 2011, 44(9), 3511 – 3516.
- [27] Yuryev Y, Wood-Adams P, Heuzey M, Dubois C, Brisson J. Crystallization study of polylactide films: An atomic force microscopy study of the effect of temperature and blending. *Polymer* 2008; 49; 2306 – 2320.
- [28] Wang H, Schultz J.M, Yan S. Study of the morphology of poly(butylene succinate)/poly(ethylene oxide) blends using hot-stage atomic force microscope. *Polymer* 2007; 48; 3530 – 3539.
- [29] Wang T, Li H, Wang F, Schultz J.M, Yan S. Morphologies and deformation behaviour of poly(vinylidene fluoride)/poly(butylene succinate) blends with variety of blend ratios and under different preparation conditions. *Polym. Chem.* 2011; 2; 1688 – 1698.
- [30] Schon P, Bagdi K, Molnar K, Markus P, Pukanszky B, Vancso GJ. *Euro Polym J* 2011; 47:692 and references cited therein.
- [31] Sinha Ray S, Bousmina M. Crystallization behaviour of poly[(butylene succinate)-*co*-adipate] nanocomposite. *Macromol Chem Phys* 2006; 207:1207–19.